2022 IEEE Photonics Society Summer Topicals Meeting Series (SUM) | 978-1-6654-3489-8/22/$31.00 ©2022 IEEE | DOI: 10.1109/SUM53465.2022.9858266

An Algorithm for Reconfigurable Coupled Resonator Optical Waveguides

Xiangfeng Chen and Wim Bogaerts
Ghent University - IMEC, Photonic Research Group, Department of Information Technology, Gent, Belgium.
Center of Nano and Biophotonics, Ghent University, Belgium.
Email: xiangfeng.chen@ugent.be

***Abstract*—We have developed an algorithm for (re)configuration of Coupled Resonator Optical Waveguides filters. We analyze in detail the effect of the phase shift introduced by tunable Mach-Zehnder interferometers. An alternating pattern is proposed to drive every other tunable coupler. We verified this algorithm to realize a user-defined all-pole filter function in circuit simulation.**

***Index Terms*—Programmable Photonics, Coupled Resonator Optical Waveguides, Tunable Coupler**

I. Introduction

Most photonic wavelength filter circuits are application-specific. With the development of integrated photonic technology, we can build complex filter circuits that can be reconfigured to different use cases without redesigning the chip [1]. Software-based training and feedback loops were reported to program user-defined transfer functions [2], [3], but a strategy based on analytical synthesis algorithms would be more scalable to higher-order, complex circuits as in Fig.1(a). The algorithmns described by Madsen and Zhao [4] provide a solid basis for configuring coupled resonator optical waveguides (CROW) circuits, consisting of a chain of ring resonators connected by directional couplers. To achieve reconfiguration, we replace the directional couplers with tunable Mach-Zehnder interferometers (MZIs), and replace the passive ring waveguides with tunable phase shifters as shown in Fig.1.

II. Tunable MZI Coupler

As shown in Fig. 1(c), every coupler has 4 ports, namely “in1”, “out1” , “in2”, “out2”. For demonstration purposes, we consider an MZI with perfect 50/50 directional couplers, thus we have a transmission matrix:

$$\begin{bmatrix} -0.5e^{-j\phi_s}+0.5e^{-j\phi_n} & -0.5je^{-j\phi_s}-0.5je^{-j\phi_n} \\ -0.5je^{-j\phi_s}-0.5je^{-j\phi_n} & 0.5e^{-j\phi_s}-0.5e^{-j\phi_n} \end{bmatrix} \quad (1)$$

We can decompose each element in the matrix (in green) into two phase vectors (phasors). These two phasors correspond to the light traveling through the North arm (in red) and the South arm (in blue). As shown in Fig.2(a-b), for light traveling from in1 to out1 in the balanced MZI, the North arm is originally at the direction (1,0) and the South arm is originally at the direction (-1,0); while for light traveling from in2 to out2, the phasors of North and South arm have the opposite direction. By tuning the phase difference between the two arms we can adjust the coupling ratio. However, it will introduce an extra phase for different light paths. For example, the extra phase is introduced due to tuning the South arm to ϕ_s for adjusting the power coupling ratio to κ. Based on this ϕ_s, we need to drive both the North and South arm together by ϕ_c as shown in Fig. 2(c-d), where $\phi_c = (\pi - \phi_s)/2$, to rotate the green vector further to (1,0) for the path in1-out1, effectively setting the phase contribution of the coupler to 0. Path in2-out2 will have the same coupling but with the phasor pointing at the opposite direction (-1,0). Here, we could tune the coupling ratio with the North arm phase shifter and commonly drive the two arms to fix the resulting phasor to (1,0) for path in2-out2, which is shown in Fig.2 (e-f). By comparison of these three MZI configurations in Fig. 2(a-f), light traveling from in1 to out1 and light traveling from in2 to out2 have intrinsic π phase difference. Flipping the North and South arm value for phase shift intrinsically introduces π of the original phasor. Those are the key operations that we will utilize in our programming strategy.

This work has received funding from the European Research Council through grant agreement No 725555 (PhotonicSWARM).

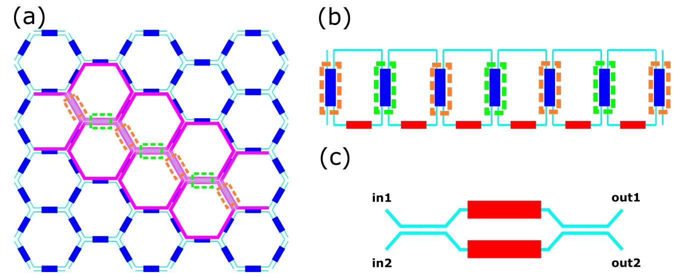

Fig. 1. (a) and (b) show CROW circuits in a hexagonal mesh and a one-dimensional chain. The blue rectangles represent tunable MZIs and the red ones are phase shifters. (c) is a schematic of a tunable MZI with two phase shifters; one in the North arm (ϕ_n) and another in the South arm (ϕ_s). Tunable couplers highlighted in orange correspond to South arm dominant phase tuning for the coupling ratio, as shown in Fig.2 (c-d). For the couplers highlighted in green the North arm has the dominant phase shift as in Fig.2 (e-f)

III. Reconfigurable Coupled Resonators

In reconfigurable CROW, passive directional couplers are replaced with the tunable MZIs and passive waveguides are replaced with the phase shifters as in Fig.1(c). For application-specific CROWs, the Madsen-Zhao algorithm is well established for the design of coupling ratios and phase shifts for a user-defined all-pole transfer function. We build our strategy on this algorithm with the spectral factorization and step-down relationship [4]. With the user-defined transfer function as in Fig. 3(a), we iteratively solve the Toeplitz matrix due to the symmetry of the linear time-invariant system, to calculate the coupling ratios of couplers and phase shifts in each ring. When we adjust the coupling ratio with tunable MZIs, the phase in two adjacent rings will also change. Fig.3 (b) shows the spectrum when we only configure it according to the coupling ratio of individual MZI without compensation of this extra phase shift. The green phasors will rotate as one of the arms is tuning the phase similar to Fig. 2(a-b). By driving the phase shifter in the North and South arm together, we introduce additional phase to effectively reset the extra phaseshift introduced by setting the coupling ratio. Fig. 3(c) is one example of such compensation when we rotate the green phasor to vector (1,0) as in Fig.2(c) for light traveling from in1 to out1 of each coupler. Because of the intrinsic π phaseshift between path in1-out1 and path in2-out2, every tunable MZI

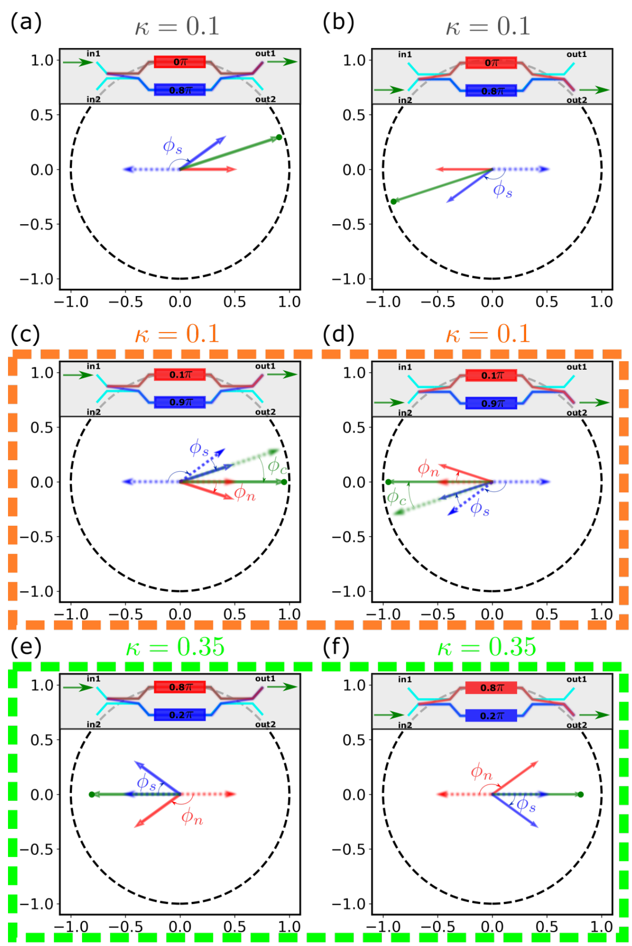

Fig. 2. Decomposition of the complex amplitude into two phase vectors (phasors) representing the North and South arm in a tunable MZI. The North arm is represented in red, and the South arm in blue. (a,c,e) illustrate the case where light travels from in1 to out1; while (b,d,f) show the transmission from in2 to out2. The coherent combination of these two beams gives us the amplitude vector in green which as the sum of the red and blue phasors.

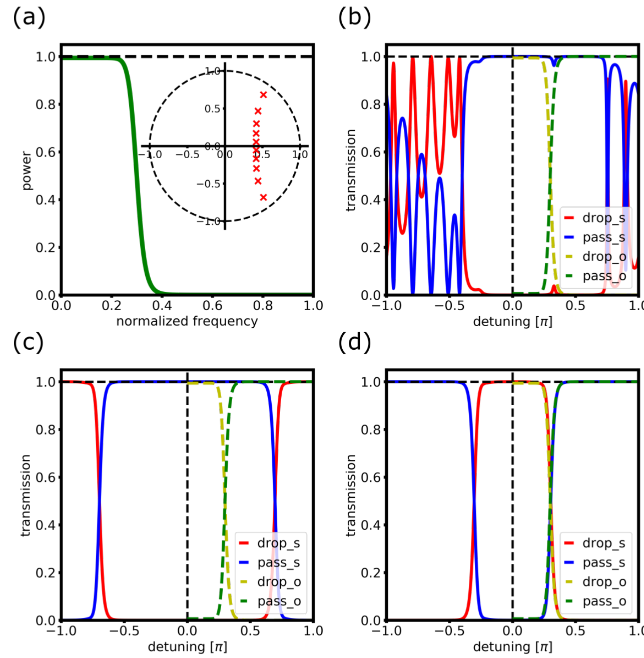

Fig. 3. (a) is an example of a typical user-defined all-pole filter response with the pole-zero plot on the upper right corner. (b) shows the effect of the extra phase introduced by setting the coupling ratio of tunable MZIs. (c) shows the spectrum after the reset of the extra phase introduced in (b) by commonly driving both phase shifters in MZI. (d) shows the synthesis result adopting alternating driving pattern; phase shift for the two arm alternates for configuration of the coupling ratio between the South arm dominant as in Fig. 2(c-d) and North arm dominant as in Fig. 2. (e-f). The transmission of the drop and pass port is compared between the original target response (with underscore o) and the result from circuit simulation of parameters from synthesis algorithms (with underscore s)

will introduce π difference between two adjacent circulating paths. We alternate the use of the North arm and South arm for the initial differential phase shift in every other coupler as indicated by the orange and green rectangles in Fig.1 and Fig.2. This way the phase difference is compensated by the fact that each ring has extra phase contributions from path in1-out1 of a coupler and path in2-out2 of another coupler. After previous steps to set the coupling ratios, the desired ring phase is then assigned to the phase shifter in the ring directly if applicable like in Fig.1 (b). Or in Fig.1 (a), the phase shift per ring is set by further commonly driving of the MZI arms in the individual ring as demonstrated in Fig. 3(d).

References

[1] D. Pérez-López, A. López, P. DasMahapatra, and J. Capmany, "Multipurpose self-configuration of programmable photonic circuits," *Nature communications*, vol. 11, no. 1, pp. 1–11, 2020.

[2] C. Lupo, D. Bunandar, D. Englund, G. R. Steinbrecher, J. Mower, J. Notaros, M. Hochberg, M. Heuck, N. C. Harris, S. Lloyd, and T. Baehr-Jones, "Programmable dispersion on a photonic integrated circuit for classical and quantum applications," *Optics Express, Vol. 25, Issue 18, pp. 21275-21285*, vol. 25, pp. 21 275–21 285, 9 2017.

[3] J. C. Mak, W. D. Sacher, T. Xue, J. C. Mikkelsen, Z. Yong, and J. K. Poon, "Automatic resonance alignment of high-order microring filters," *IEEE Journal of Quantum Electronics*, vol. 51, 11 2015.

[4] C. K. Madsen and J. H. Zhao, *Optical filter design and analysis*. Wiley New York, 1999.